Enhanced marrow adipogenesis and bone resorption in estrogen-deprived rats treated with the PPARgamma agonist BRL49653 (Rosiglitazone)

Virginie Sottile, Klaus Seuwen, and Michaela Kneissel

Corresponding author:

Klaus Seuwen, PhD
Novartis Pharma AG
Research, Bone Metabolism
WK-125.9.13
CH-4002 Basel
Switzerland
Tel.: +41 61 696 1951
Fax: +41 61 696 3849
e-mail: klaus.seuwen@pharma.novartis.com

Abstract

Osteoporosis is characterized by loss of bone tissue and increased bone marrow fat content. Since osteoblasts and adipocytes originate from a common mesenchymal precursor cell, it has been proposed that osteoporosis might in part result from a switch of cell differentiation favoring adipogenesis. We tested this hypothesis by evaluating the effect of the thiazolidinedione BRL49653 (Rosiglitazone), a potent stimulator of adipogenesis acting through the nuclear hormone receptor PPARgamma, on bone tissue and marrow of intact and estrogen-deprived female rats.

In a first step skeletally mature intact rats were treated for 8 weeks with 5, 10, or 20 mg/kg of BRL49653 or vehicle. Increased body weight and decreased plasma triglyceride levels confirmed the effectiveness of the treatment. No change in bone mass or fat marrow volume was observed as evaluated by DEXA, pQCT, and histomorphometry. However, the study of marrow cultures established at necropsy revealed a significantly higher responsiveness to adipogenic treatment of cultures established from the 10 mg/kg group compared to vehicle control.

We then studied rats that had been estrogen-deprived by ovariectomy (OVX). Treatment with the 10 mg/kg dose for 12 weeks resulted in a significantly increased bone loss (+31% based on pQCT), compared to vehicle-treated OVX animals. Histomorphometric evaluation of tibias taken at necropsy revealed that the fat marrow volume, which had increased 4.6-fold upon OVX, compared to sham control, was increased more than 10-fold in the treatment group. Interestingly, osteoblast number was comparable in vehicle and BRL49653-treated OVX animals, though lower than in SHAM controls. Bone resorption parameters were significantly increased in the treatment group (+27% osteoclast number, +30% eroded surface).

Our data demonstrate that the thiazolidinedione BRL49653 has the potential to potentiate bone loss stimulated by estrogen deprivation. The skeleton of intact animals remained unaffected, suggesting that an estrogen-dependent control mechanism protects bone from catabolic signals elicited by activated PPARgamma.

Introduction

The bone marrow contains mesenchymal precursor cells giving rise to both osteoblasts and adipocytes (Pittenger [1], Krebsbach [2]). A deregulation of precursor cell differentiation may be involved in the pathology of osteoporosis, since several reports associate the degradation of the bone structure and a concomitant increase of bone marrow fat content (Meunier [3], Burkhardt [4], Minaire [5]). Following these observations, the hypothesis was formulated that during developing osteopenia adipocyte recruitment might occur at the expense of osteoblast development.

The thiazolidinediones (TZDs) are antidiabetic compounds that were discovered to be potent stimulators of adipogenesis. These molecules sensitize target tissues to the action of insulin, and therefore are widely used clinically to treat type II diabetes. TZDs bind and activate the nuclear receptor PPARgamma, which exerts critical control over the adipocyte differentiation process (Lehmann [6], Rosen [7], Spiegelman [8]). TZDs are routinely used today in adipogenic treatment protocols to induce fat droplet accumulation within few days in mesenchymal precursor cultures (Gimble [9], Sottile [10]).

In vitro cell differentiation studies indeed indicated that TZDs inhibit osteogenic differentiation, while favoring adipogenic conversion of precursor cells ( ). However, the potential impact of TZDs on bone status *in vivo* is only poorly documented, despite the obvious importance of the question given the widespread clinical use of these molecules for the treatment of type II diabetes.

An early animal study, which is so far only published in abstract form (*Jennermann 1995 [13]*), reported a significant reduction of tibia BMD in rats treated for 28 days with pioglitazone. In contrast, Tornvig et al. reported recently increased bone marrow adipose tissue, but normal bone status, in mice following a 10-month treatment with troglitazone ( ). The authors concluded that adipogenesis and osteogenesis are regulated independently in bone marrow.

We describe here a study carried out with skeletally mature female rats, investigating also the impact of TZD treatment on bone loss following ovariectomy. Our data support in part the results presented by Tornvig et al, in that no deleterious effect of TZD treatment on bone status could be detected in intact animals. However, a significant acceleration of bone loss could be measured upon estrogen deprivation, which appears due to increased bone resorption.

(Not cited in introduction:
Okazaki [14], ocs in vitro / Deldar [16] dog.)

Material and Methods

Animals

Wistar rats (BRL, Fuellingsdorf, Switzerland) were housed in groups of five animals at 25°C with a 12:12 h light-dark cycle. They were fed a standard laboratory diet containing 0.8% phosphorus and 1.1% calcium (NAFAG 890, Basel, Switzerland). Food and water was provided *ad libitum*.

Study Design

Skeletally mature 6 month old intact female virgin rats were used in the first study. The rats were evenly distributed into 4 groups according to body weight and cross-sectional total bone mineral density in the tibia as measured at baseline by pQCT (n=8/group). The animals were treated daily for 8 weeks with BRL49653 (produced at Novartis, Basel) at doses of 5, 10, or 20 mg/kg/day or vehicle (1% carboxy-methylcellulose) by gavage. Changes in bone density (DEXA, pQCT) were evaluated *in vivo* after four weeks of treatment and at eight weeks before necropsy and compared to baseline values.

In the second study a similar protocol was used on 9 month old skeletally mature estrogen-deficient rats (n=8/group). Bilateral ovariectomy (OVX) was carried out in all animals by a dorso-lateral approach under inhalation anaesthesia using Forene® (isoflurane, WOB506, Lot 55370VA, Abbott AG, Switzerland) with the exception of a SHAM-operated group. Animals were treated for 12 weeks daily with BRL 49653 (10 mg/kg/day) or vehicle by gavage. Changes in bone mass and geometry (DEXA, pQCT) were evaluated *in vivo* after four and eight weeks of treatment and at twelve weeks before necropsy and compared to baseline values.

Body weight was monitored weekly in both studies. Blood was taken at necropsy. DEXA measurements were carried out after necropsy on excised tibia, femur, and lumbar vertebrae. One tibia was processed for histomorphometric analysis.

DEXA measurements

Bone mineral density (mg/cm^2) of the proximal quarter of the left tibia was measured using a regular Hologic QDR-1000 instrument (Hologic, Waltham, MA, USA) adapted for measurements of small animals. A collimator with 0.9 cm diameter and an ultrahigh resolution mode (line spacing 0.0254 cm, resolution 0.0127 cm) were used.

During the measurements, the animals were put under inhalation narcosis (isoflurane, 2.5%) on a resin platform provided by the company for soft tissue calibration. The animals were placed in supine position. Their hind limbs were maintained in external rotation with a tape. Hip, knee and ankle were in 90° flexion. The left tibia was measured in total and in the proximal quarter. To control the stability of the measurements, a phantom was scanned daily.

For *ex vivo* experiments, the left tibia, femur, and the lumbar vertebrae 1-4 were collected at necropsy and put in [* is there something missing here ?] over night. In the DEXA measurements 70% ethanol was used for soft tissue simulation.

pQCT measurements

Cross-sectional bone mineral density (mg/cm^3) was monitored in the proximal tibia metaphysis 4.5 mm distal from the intercondylar tubercle using an adapted Stratec-Norland XCT-2000 (Pforzheim, Germany) fitted with an Oxford 50 microM X-ray tube (Oxford GTA6505M/LA, UK) and a collimator of 1 mm diameter. The following setup was chosen for the measurements: voxel-size: 0.2 mm x 0.2 mm x 1 mm, scan speed: scout view 20 mm/s, final scan 10mm/s, 1 block, contour mode 1, peel mode 2, cortical threshold 610 mg/cm^3, inner threshold 610 mg/cm^3.

The animals were placed in a lateral position under inhalation narcosis (isoflurane, 2.5%). The left leg was stretched and fixed in this position.

Blood sampling

Blood samples of 500µl were taken in heparin at necropsy. Triglyceride levels were determined on a COBAS MIRA S system (Roche Diagnostics, Rotkreuz, Switzerland) using the standard test kits and calibration standards provided by Roche Diagnostics.

Tissue processing and histomorphometric analysis

The proximal right tibia was fixed at 4°C (Karnovsky fixative) for 24 hour, dehydrated, defattened and embedded in resin (HistoDur Leica, Nussloch, Germany). A set of 4 and 10µm non consecutive microtome sections was cut (Microtome 2050 Supercut, Reichert Jung, Germany) in the frontal mid-body plane. ~~of~~ Structural and cellular parameters were evaluated using a Leica DM microscope (Leica, Switzerland) fitted with camera (SONY DXC-950P, Japan) and adapted Quantimet 600 software (Leica, Cambridge, U.K.).

Three sections per animal were sampled for all sets of parameters. The mineralized bone at the 10µm section surface was silver-stained with modified von Kossa stain thus facilitating the determination of static structural bone parameters. Images of the stained mineralized surface layer were taken and converted into binary images. Bone volume per tissue volume (%), trabecular width (µm), trabecular number (mm-1) and trabecular separation (µm) were determined at 50x according to the plate model (Parfitt et al. 1987) in the secondary spongiosa of the proximal tibia metaphysis. The 4µm thick sections were stained with modified Giemsa stain or tartrate-resistant acid phosphatase (TRAP) for evaluation of fat cell area and bone turnover <better fat cell and osteoclast number ?>. Microscopic images of the specimen were either evaluated using ~~a using~~ a Merz grid (fat marrow content) or digitized and evaluated semi-automatically on screen (bone turnover; 200x). Fat volume per marrow volume (%) and

osteoblast number (Obl.N / B.Pm (mm-1)) were measured on the Giemsa stained sections, while osteoclast number (Ocl.N / B.Pm (mm-1)) was determined on the TRAP stained slides. All measurements were carried out according to the recommendation of Parfitt et al. [17].

Statistical analysis

Results are expressed as mean ± SEM. Statistical analysis was carried out using BMDP (Version 1990 for VAX/VMS, BMDP Statistical Software Inc., Cork Ireland) for the study on intact animals containing three doses of the compound. The data were subjected to one-way analysis of variance (ANOVA). Equality of variances was tested by Levene F-test and differences between groups using the Bonferroni-adjusted Dunnett test (significance level: $p<0.05$). The treated groups were tested for difference from the vehicle-treated intact control group. In the study on estrogen-deficient animals, where only one dose of BRL49653 was applied, statistical analysis was carried out using Student t-test (Microsoft Excel). All statistical tests were two-tailed and unpaired. * = p<.05 Vehicle, Vehicle SHAM ⇔ BRL49653, x = p<.05 Vehicle OVX ⇔ BRL49653, ** = p<.01 Vehicle (SHAM) ⇔ BRL49653, xx = p<.01 Vehicle (OVX) ⇔ BRL49653

Bone marrow cell culture

Fine chemicals were purchased from Sigma (Buchs, Switzerland) unless otherwise stated.

At necropsy, bone marrow was prepared immediately from the left tibia and femur of each animal. Cells from each treatment group were pooled. Cell cultures were established in MEMalpha/Ham's F12 medium (Life Technologies, Basel, Switzerland) supplemented with 10% fetal bovine serum (Bioconcept, Allschwill, Switzerland) and antibiotics (Bioconcept). The seeding density for primary cultures was 1.5 x 10^8 cells per T175 flask. After 4 days in primary culture, non-adherent cells were removed by medium change, and cfu / cm^2 were determined. Cultures were maintained until they reached confluence (day 16) with medium change every third day. The cultures were then split 1:4 (passage 1), grown to confluence, and part of the cells were seeded for differentiation assays, while the remaining cells were frozen for later analysis.

Osteogenic differentiation

Cells were seeded in 12-well plates at a density of 20'000 cells per well and grown for 4 days. Osteogenic medium was then added (normal medium supplemented with ascorbic acid (50 microM), beta-glycerophosphate (10 mM), and calcium adjusted to 1.8 mM final). Cultures were maintained for 21 days (medium change twice weekly) before calcium deposited in wells was determined using the MPR2 assay kit (Roche Diagnostics).

Adipogenic differentiation

Cells were seeded in 6-well plates at a density of 400'000 cells per well and grown for 4 days. Adipogenic medium was then added (normal medium supplemented with isobutylmethylxanthine (0.2 mM) and BRL49653 (1 microM)). Cultures were maintained for 12 days (medium change twice weekly) before determination of adipocyte numbers (Oil Red O stain and flow cytometry).

Determination of adipocyte numbers

Flow cytometry using the lipophilic dye Nile Red was carried out as described by Gimble et al [9]. Cells were trypsinized, washed with PBS, and fixed with 4% paraformaldehyde at 4ºC. Cells were then resuspended in PBS with a final concentration of Nile Red of 1mg/ml, and kept on ice for 30min. The samples were analysed with a FACScan^{TM} flow cytometer (Becton Dickinson, Basel, Switzerland). Nile Red fluorescence was measured on the FL-2 emission channel through a 580 ± 21nm band pass filter following excitation with an argon ion laser source at 488nm. We used the FL-2 / forward scatter (FSC) plot of events to define a selection window called R2 in which cells with high FL-2 values were counted (adipocytes). For each sample 20000 events were collected. The results are expressed as the percentage of cells appearing in the R2 region. All determinations were done in duplicate.

GPDH activity assay

For biochemical determination of GPDH activity cell extracts were prepared in Tris/EDTA buffer. Aliquots were incubated at 37^{o}C in 1 ml of assay solution containing 0.1 M triethanolamine, 2.5 mM EDTA, 0.1 mM beta-mercaptoethanol, 125 mM NADH (Roche Diagnostics) and 200 mM dihydroxyacetonephosphate. Enzyme activity is reflected by the disappearance of NADH measured by absorption at 340 nm over 10 - 20 min. The protein content of each sample was analyzed in parallel using the BioRad $^{D}_{C}$Protein Assay (BioRad, Glattbrugg, Switzerland). Results are expressed as mU / mg protein, 1 mU being defined as 1 nmol NADH reacted / min. All determinations were done in duplicate.

Results

Intact animals receiving BRL49653 gained weight and showed a significant reduction of plasma triglyceride levels with dose, as expected with such treatment (Fig.1 A, B). However, bone mineral density, as evaluated by DEXA in the entire proximal tibia and by pQCT in a proximal metaphyseal cross section, remained unchanged over the 8-week period (Fig.1C, D). Similarly, no effect was observed on bone mineral density values in the femur and in lumbar vertebral bodies as evaluated *ex vivo* by DEXA (data not shown). Histomorphometric analysis of the tibial cancellous bone structure confirmed these findings and did not reveal differences between vehicle and BRL49653-treated animals (Fig. 2A and data not shown). Fat marrow volume was low in the proximal tibia metaphysis in these 9-month old animals. It appeared slightly higher in the treatment groups compared to control, however, these differences did not reach statistical significance (Fig. 2B).

In mesenchymal cell cultures isolated from the bone marrow of these animals after necropsy, colony formation capacity appeared slightly reduced for the BRL49653-treated groups at 5 and 10 mg/kg, a significant reduction of about 50% was observed for the 20 mg/kg group (Fig. 3A). However, following equal expansion of cell cultures at passage 1, exposure to osteogenic conditions induced strong mineral deposition in cultures from all treatment groups (Fig. 3B). Quantification of mature adipocytes following adipogenic differentiation using Nile Red flow cytometry revealed a significant increase in adipocyte numbers in cultures established from animals treated with 10 mg/kg of BRL49653. Biochemical determination of GPDH activity produced similar results, albeit less pronounced (Fig. 4).

Following this first series of experiments with intact animals we carried out a second study aimed at evaluating the effects of TZD treatment on bone status following ovariectomy. Estrogen deprivation induced the expected increase in body weight over the 12-week treatment period (Fig. 5A). This increase was further enhanced in the group receiving BRL49653. The significant drop of triglyceride levels in animals receiving the TZD confirmed the effectiveness of the treatment (Fig. 5B). Measurements of bone mineral density showed the expected significant bone loss induced by ovariectomy from the first scanning time point onwards. This bone loss was significantly enhanced in OVX animals treated with BRL49653 from the 8-week measurement point onward (Fig. 1C, D). PQCT detected a 30% increased loss of total bone mineral density (Fig.1D). Potentiation of bone loss occurred both in the cancellous and cortical compartment (cancellous BMD OVX/vehicle =: -41.1 % ± 2.4 versus OVX/BRL49653= -48.5 % ± 2.4, $p<.05$; cortical bone mineral content at week 12 OVX/vehicle =: -18.2 % ± 1.7 versus OVX/BRL49653= -24.0 % ± 2.0, $p<.05$). The latter was due to endocortical bone loss (endocortical circumference OVX/vehicle =: 33.0 % ± 5.2 versus OVX/BRL49653= 44.1 % ± 3.7, $p<.1$).

Ex vivo DEXA measurements of bone mineral density demonstrated that a similar effect had occurred in the femur (OVX/vehicle =: 264 mg/cm^2 ± 5 versus OVX/BRL49653 = 249 mg/cm^2 ± 5, p<.05) and in the lumbar spine (OVX/vehicle =: 236 mg/cm^2 ± 4 versus OVX/BRL49653= 208 mg/cm^2 ± 4, p<.01).

Histomorphometric analysis of the secondary spongiosa in the proximal tibia metaphysis again confirmed that cancellous bone volume was significantly reduced following ovariectomy (Fig. 6A). This was more pronounced in BRL49653-treated animals. The typical structural changes due to estrogen loss were observed: Trabecular number was significantly decreased (Fig. 6B) and separation significantly increased (Fig. 6D), while trabecular thickness was only mildly decreased (Fig. 6C). The potentiation of these structural changes in response to BRL49653 treatment was visible in all three measured parameters (Fig.6A-C).

Fat marrow volume was slightly higher in the 12-month old vehicle-treated intact animals (Figs. 6E, 7A) compared to the 3-month younger intact control animals of the first study (Fig. 2B). As expected, estrogen deficiency resulted in an increased in fat marrow content (4.6-fold; Fig. 6E, 7B). This was significantly enhanced in the PPARgamma agonist-treated rats (10-fold; Fig. 6E). A substantial number of apparently mature adipocytes was visible (Fig. 7C). Osteoblast number was lower in estrogen-deficient animals (Fig. 6F), but no difference was observed between vehicle and BRL49653-treated rats. Osteoclast number (Fig. 6G) and eroded bone surface (Fig. 6H) was not different between vehicle-treated SHAM and OVX animals. Taken together with the data for osteoblast number, this suggests that bone turnover was not increased anymore at this late stage of estrogen deficiency. However, both parameters were still significantly increased in the estrogen-deficient animals receiving the TZD (+27% osteoclast number, Fig. 6G; +30% eroded surface, Fig. 6H).

Discussion

Treatment of intact adult rats with the TZD BRL49653 did not lead to increased fat cell differentiation in the bone marrow, and no adverse effects on bone status could be measured. However, body weight increased in treated animals and plasma triglyceride levels were lowered, clearly demonstrating that the treatment was effective. Likewise, increased *in vitro* adipogenic differentiation of first passage bone marrow mesenchymal cell cultures established from TZD-treated animals confirmed that the TZD was active.

Our observations contradict the results of a comparable study published in abstract form, where a 4-week administration of pioglitzone had led to a significant loss of bone mineral density [Jennermann [13]]. Also, our results appear in conflict with a dog study, reporting an increased fat content in bones following TZD treatment [Deldar [16]]. Recently, the effects of treating apolipoprotein E (apoE)- deficient mice with troglitazone for a prolonged time (10 months) were reported [Kassem]. At the end of the treatment these animals showed strongly increased adipose tissue volume in the proximal tibia compared to control animals, however, no change of bone volume per total volume was observed in histomorphometric experiments. These data led the authors to conclude that adipogenesis and osteogenesis are regulated independently in the bone marrow. This study is in good agreement with our results with intact rats regarding overall bone status. The increased marrow fat content may be attributed to the very long treatment phase (almost life-long). Unfortunately, the deficiency in apoE of the animals employed makes a direct comparison with our data difficult, especially as apoE may be involved in the regulation of bone mineral density [Salamone LM JBMR2000].

No data were previously available regarding TZD effects on bone in estrogen-deficient animals. We observed that treatment of ovariectomised rats with BRL49653 significantly enhanced bone loss and bone marrow fat content. Given the results described above for intact animals, these results were unexpected. Interestingly, the increased marrow fat content was not paralleled by a decrease in osteoblast number as determined by histomorphometry, which is in line with the conclusion drawn by [Kassem]. It indicates that despite increased adipogenic differentiation, the stem cell pool available for osteoblastic differentiation in the marrow is not critically depleted. This observation is also in line with other data from our laboratory showing that TZDs do not necessarily block osteogenic differentiation of precursor cells [Sottile submitted].

The increased bone loss observed in ovariectomised animals treated with BRL49653 rather seems to be due to accelerated resorption. Thus, osteoclast number and eroded surface per bone surface were significantly increased in the TZD-treated group. At first sight this result is again unexpected, as several recent reports demonstrated inhibition of osteoclast differentiation

by PPARgamma agonists *in vitro* [Okazaki Endocrinology 1999, Mbalaviele JBC 2000, Bendixen PNAS 2001]. However, the *in vivo* context is undoubtedly more complex and obviously permissive for other types of regulation. It should also be noted that rather high concentrations of PPARgamma agonists were required in the cited *in vitro* studies to induce inhibition of osteoclast differentiation [<I have to check again>

For TZD compounds :

Okazaki 1999 uses 10uMBRL, but most of the in vitro data are based on troglitazone 3-30uM

Mbalaviele 2000 uses ciglitazone 10-50uM

Bendixen 2001 uses ciglitazone 3-30uM].

In summary, …

Estrogen-dependent or not, add challenge question to outlook?

Acknowledgements

We thank Barbara Wilmering for support in cell culture. Anne Studer, Margot Brüderlin, and Reto Cortesi are gratefully acknowledged for their essential contributions to the *in vivo* aspects of this study.

References <not up to date>

1. Pittenger MF, Mackay AM, Beck SC, Jaiswal RK, Douglas R, Mosca JD, Moorman MA, Simonetti DW, Craig S, Marshak DR (1999) Multilineage potential of adult human mesenchymal stem cells. *Science* 284: 143-147.

2. Krebsbach PH, Kuznetsov SA, Bianco P, Robey PG (1999) Bone marrow stromal cells: characterization and clinical application. *Crit Rev Oral Biol Med* 10: 165-181.

3. Meunier P, Aaron J, Edouard C, Vignon G (1971) Osteoporosis and the replacement of cell populations of the marrow by adipose tissue. *Clin Orthop Rel Res* 80: 147-154.

4. Burkhardt R, Kettner G, Bohm W, Schmidmeier M, Schlag R, Frisch B, Mallmann B, Eisenmenger W, Gilg T (1987) Changes in trabecular bone, hematopoiesis and bone marrow vessels in aplastic anemia, primary osteoporosis, and old age: a comparative histomorphometric study. *Bone* 8: 157-164.

5. Minaire P, Edouard C, Arlot M, Meunier PJ (1984) Marrow changes in paraplegic patients. *Calcif Tissue Int* 36: 338-340.

6. Lehmann JM, Moore LB, Smith-Oliver TA, Wilkison WO, Willson TM, Kliewer SA (1995) An antidiabetic thiazolidinedione is a high affinity ligand for peroxisome proliferator-activated receptor gamma (PPAR gamma). *J Biol Chem* 270: 12953-12956.

7. Rosen ED, Walkey CJ, Puigserver P, Spiegelman BM (2000) Transcriptional regulation of adipogenesis. *Genes Dev* 14: 1293-1307.

8. Spiegelman BM (1998) PPAR-gamma : adipogenic regulator and thiazolidinedione receptor. *Diabetes* 47: 507-514.

9. Gimble JM, Robinson CE, Wu X, Kelly KA, Rodriguez BR, Kliewer SA, Lehmann JM, Morris DC (1996) Peroxisome proliferator-activated receptor-gamma activation by thiazolidinediones induces adipogenesis in bone marrow stromal cells. *Mol Pharmacol* 50: 1087-1094.

10. Sottile V, Seuwen K (2000) Bone morphogenetic protein-2 stimulates adipogenic differentiation of mesenchymal precursor cells in synergy with BRL 49653 (rosiglitazone). *FEBS Lett* 475: 201-204.

11. Lecka-Czernik B, Gubrij I, Moerman EJ, Kajkenova O, Lipschitz DA, Manolagas SC, Jilka RL. (1999) Inhibition of Osf2/Cbfa1 expression and terminal osteoblast differentiation by PPARgamma2. *J Cell Biochem* 74: 357-371.

12. Jackson SM, Demer LL. Peroxisome proliferator-activated receptor activators modulate the osteoblastic maturation of MC3T3-E1 preosteoblasts. *FEBS Lett* 471: 119-124.

13. Jennermann C, Triantafillou J, Cowan D, Pennink BGA, Connolly KM, Morris DC (1995) Effects of the thiazolidinediones on bone turnover in the rat. *J Bone Min Res* 10: 5241.

14. Okazaki R, Toriumi M, Fukumoto S, Miyamoto M, Fujita T, Tanaka K, Takeuchi Y (1999) Thiazolidinediones inhibit osteoclast-like cell formation and bone resorption in vitro. *Endocrinology* 140: 5060-5065.

15. Tornvig L, Justesen J, Mosekilde L, Falk E, Kassem M (2001) Troglitazone treatment induces bone marrow adipose tissue volume but does not affect trabecular bone volume in mice. *Calcif Tissue Int* 69: 46-50.

16. Deldar A, Williams G, Stevens C (1993) Pathogenesis of thiazolidinedione-induced hematotoxicity in the dog. *Diabetes* 42(suppl.): 179.

17. Parfitt AM, Drezner MK, Glorieux FH, Kanis JA, Malluche H, Meunier PJ, Ott SM, Recker RR (1987) Bone histomorphometry: standardization of nomenclature, symbols, and units. Report of the ASBMR Histomorphometry Nomenclature Committee. *J Bone Miner Res* 2: 595-610.

18. Park SR, Oreffo RO, Triffitt JT (1999) Interconversion potential of cloned human marrow adipocytes in vitro. *Bone* 24: 549-554.

19. Bennett JH, Joyner CJ, Triffitt JT, Owen ME (1991) Adipocytic cells cultured from marrow have osteogenic potential. *J Cell Sci* 99: 131-139.

20. Zhang B, Graziano MP, Doebber TW, Leibowitz MD, White-Carrington S, Szalkowski DM, Hey PJ, Wu M, Cullinan CA, Bailey P, Lollmann B, Frederich R, Flier JS, Strader CD, Smith RG (1996) Down-regulation of the expression of the obese gene by an antidiabetic thiazolidinedione in Zucker diabetic fatty rats and db/db mice. *J Biol Chem* 271: 9455-9459.

Figure Legends

Figure 1

Weight gain (A) and plasma triglyceride levels (B) after 8 weeks of treatment of skeletally mature intact female Wistar rats. (C) Bone mineral density in the proximal tibia as determined by DEXA measurements. (D) Change in cross-sectional bone mineral density in the tibial metaphysis from baseline value as measured by peripheral quantitative computed tomography (pQCT). Mean ± SEM, ANOVA. **p<.01 vehicle ⇔ BRL49653. Small caps on bars indicate measurements at baseline (a) and after 4 and 8 weeks of treatment (b, c, respectively).

Figure 2

Histomorphometric analysis of cancellous bone (A) and fat marrow (B) volume in the proximal tibia metaphysis of vehicle and BRL49653-treated animals. Results are expressed as Mean ± SEM, ANOVA.

Figure 3

Analysis of marrow mesenchymal cell cultures established at necropsy. Colony formation capacity (A) was evaluated in each culture 4 days after cell isolation. Mineral deposition in passage 1 cultures (B) was measured after 21 days under control (white bars) or osteogenic conditions (shaded bars). Mean ± range of duplicate determinations.

Figure 4

Adipogenic differentiation of marrow mesenchymal cells. Cultures were treated under control or adipogenic conditions for 12 days. Representative photomicrographs and dot-plots from flow cytometry are shown in (A). Bar = 50microm. Corresponding quantitative results from flow cytometry are presented in (B); data from enzymatic dosage of GPDH activity in (C). White bars indicate control, solid bars indicate adipogenic treatment of cell cultures. Mean ± range of duplicate determinations.

Figure 5

Weight gain (A) and plasma triglyceride levels (B) after 12 weeks of treatment of skeletally mature SHAM operated and ovariectomized (OVX) vehicle and BRL49653 treated female Wistar rats. (C) Bone mineral density in the proximal tibia as determined by DEXA. (D) Change in cross-sectional bone mineral density in the tibial metaphysis from baseline as measured by pQCT. Mean ± SEM, t-test, * p<.05, ** p<.01 vehicle SHAM ⇔ vehicle OVX, BRL49653 OVX, x p<.05, xx p<.01 vehicle OVX ⇔ BRL49653 OVX. Small caps on bars indicate measurements at baseline (a) and after 4, 8, and 12 weeks of treatment (b, c, d, respectively).

Figure 6

Cancellous bone volume (A), trabecular number (B), trabecular thickness (C), trabecular separation (D), fat marrow volume (E), osteoblast number (F), osteoclast number (G), and eroded surface (H) in the proximal tibia metaphysis of skeletally mature SHAM operated and ovariectomized (OVX) vehicle and BRL49653 treated female Wistar rats. Mean ± SEM, t-test, * p<.05, ** p<.01 vehicle SHAM ⇔ vehicle OVX, BRL49653 OVX, x p<.05, xx p<.01 vehicle OVX ⇔ BRL49653 OVX

Figure 7

Secondary spongiosa and bone marrow on a Giemsa stained section (200x) from a (A) vehicle treated SHAM animal, (B) vehicle treated OVX animal, and (C) BRL49653 (10mg/kg) treated OVX animal. Note the increasing volume of mature adipocytes from A to C (green arrows).

Figure 1

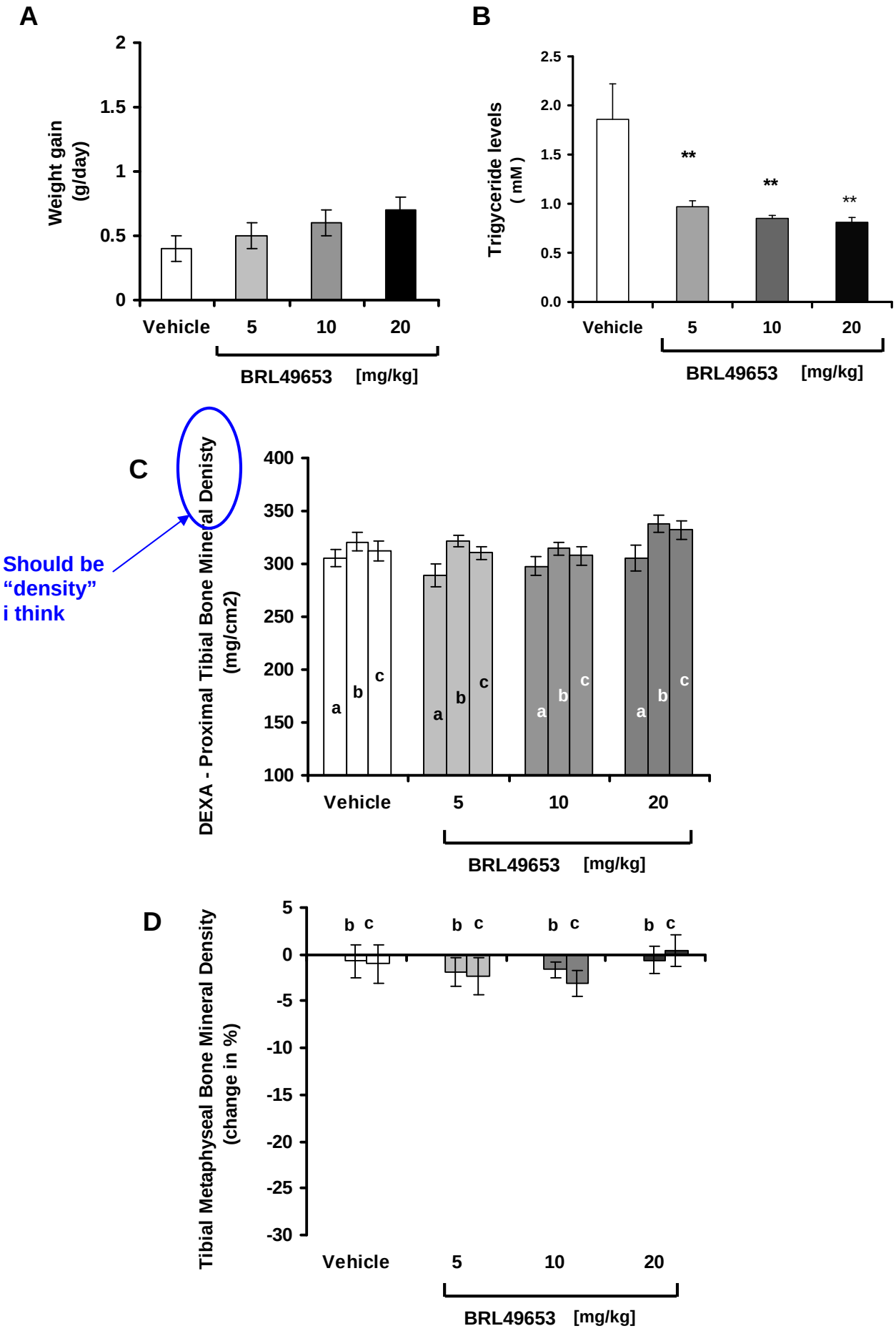
A
Weight gain (g/day)
2
1.5
1
0.5
0
Vehicle
5
10
20
BRL49653 [mg/kg]
B
Trigyceride levels (mM)
2.5
2.0
1.5
1.0
0.5
0.0
**
**
**
Vehicle
5
10
20
BRL49653 [mg/kg]
C
Should be "density" i think
DEXA - Proximal Tibial Bone Mineral Denisty (mg/cm2)
400
350
300
250
200
150
100
a
b
c
Vehicle
5
10
20
BRL49653 [mg/kg]
D
Tibial Metaphyseal Bone Mineral Density (change in %)
5
0
-5
-10
-15
-20
-25
-30
b c
Vehicle
5
10
20
BRL49653 [mg/kg]

Figure 2

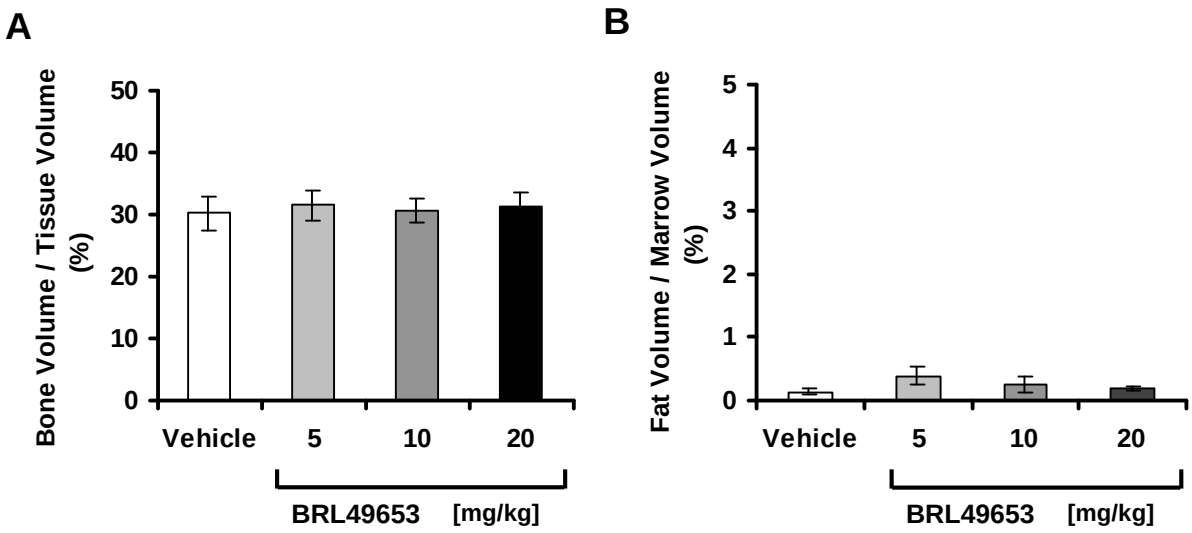
A
Bone Volume / Tissue Volume (%)
50
40
30
20
10
0
Vehicle
5
10
20
BRL49653 [mg/kg]
B
Fat Volume / Marrow Volume (%)
5
4
3
2
1
0
Vehicle
5
10
20
BRL49653 [mg/kg]

Figure 3

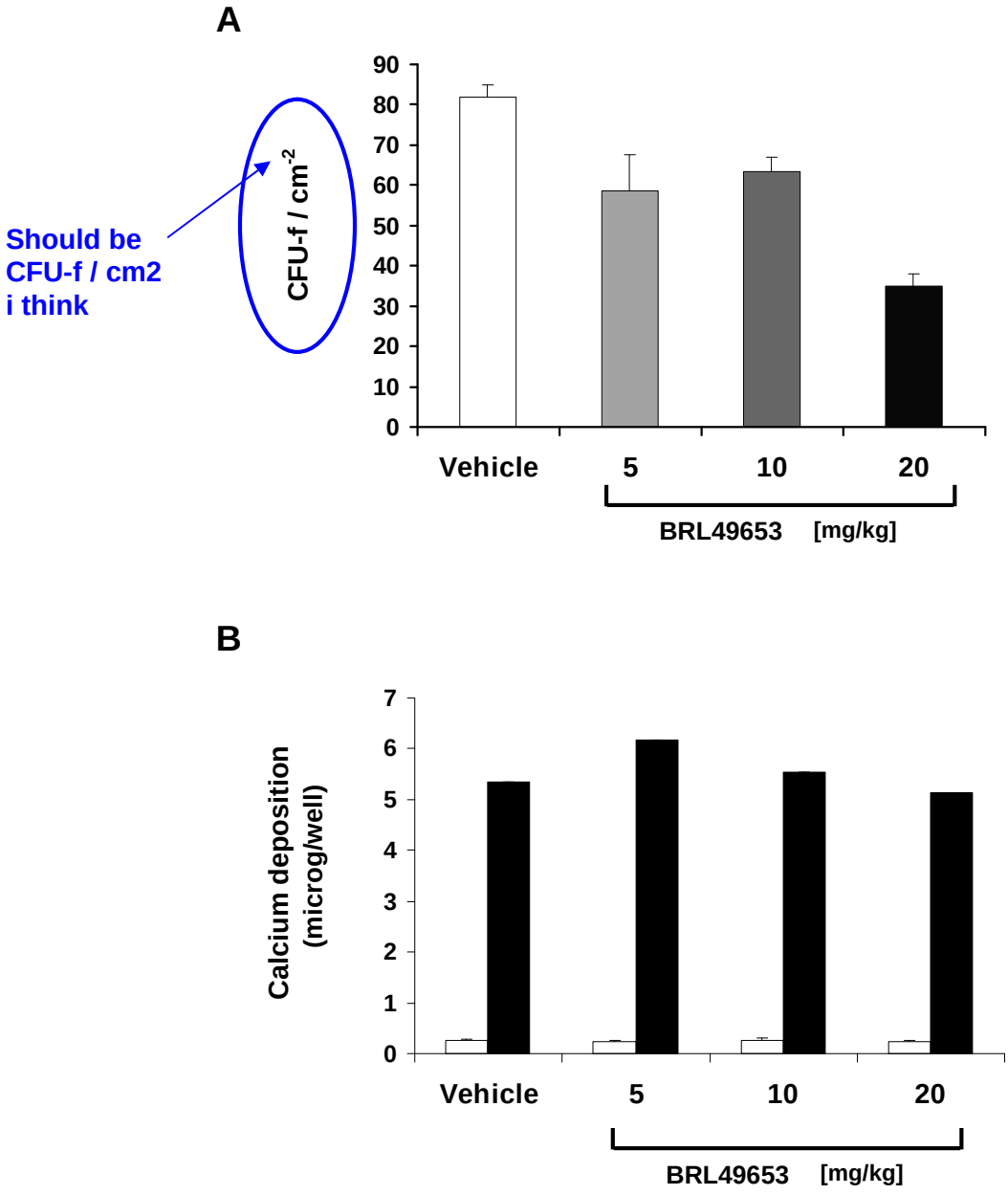
A
Should be
CFU-f / cm2
i think
CFU-f / cm-2
90
80
70
60
50
40
30
20
10
0
Vehicle
5
10
20
BRL49653 [mg/kg]
B
Calcium deposition
(microg/well)
7
6
5
4
3
2
1
0
Vehicle
5
10
20
BRL49653 [mg/kg]

Figure 4

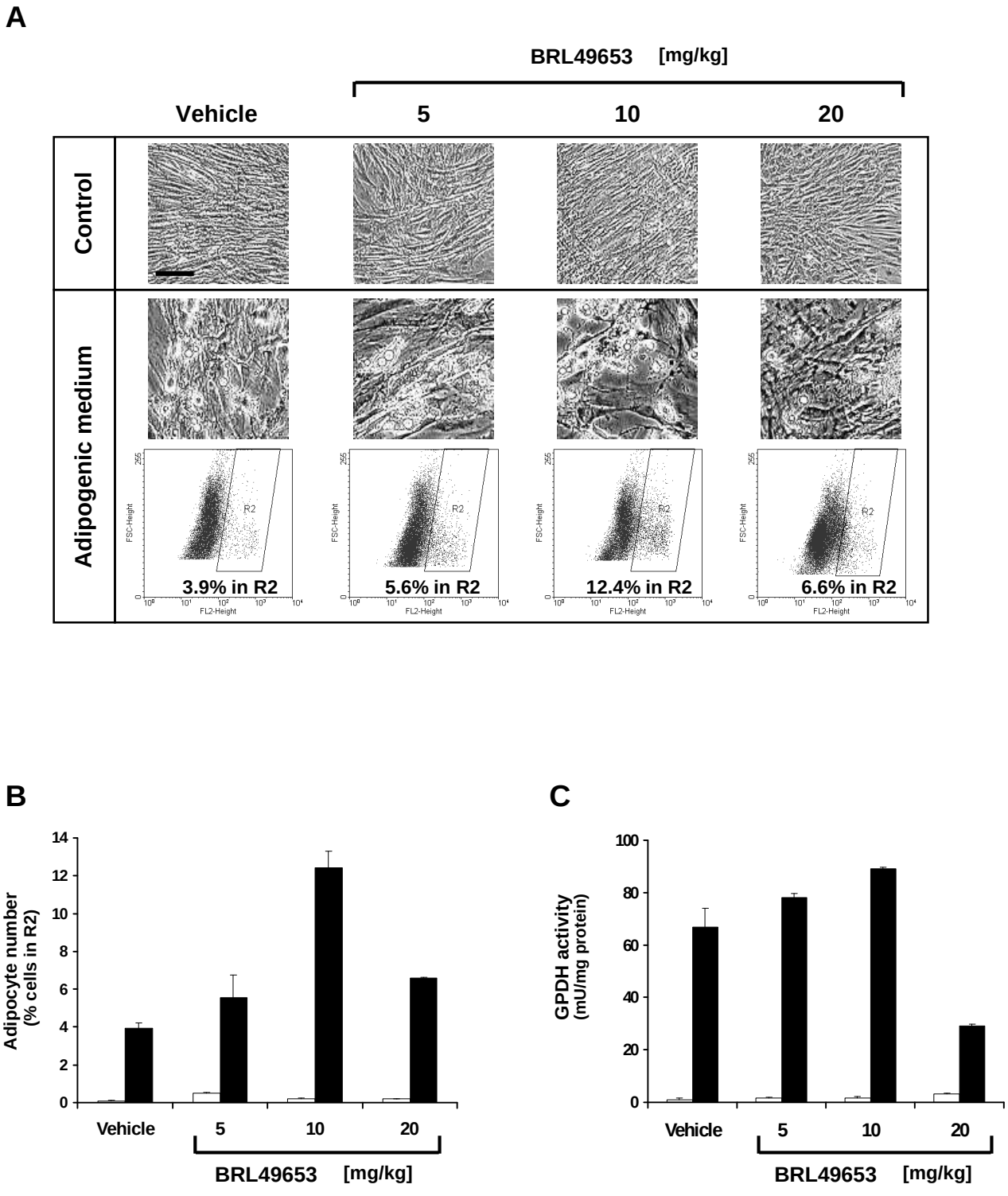
A
BRL49653 [mg/kg]
Vehicle
5
10
20
Control
Adipogenic medium
FSC-Height
FL2-Height
R2
3.9% in R2
5.6% in R2
12.4% in R2
6.6% in R2
B
Adipocyte number (% cells in R2)
Vehicle
5
10
20
BRL49653 [mg/kg]
C
GPDH activity (mU/mg protein)
Vehicle
5
10
20
BRL49653 [mg/kg]

Figure 5

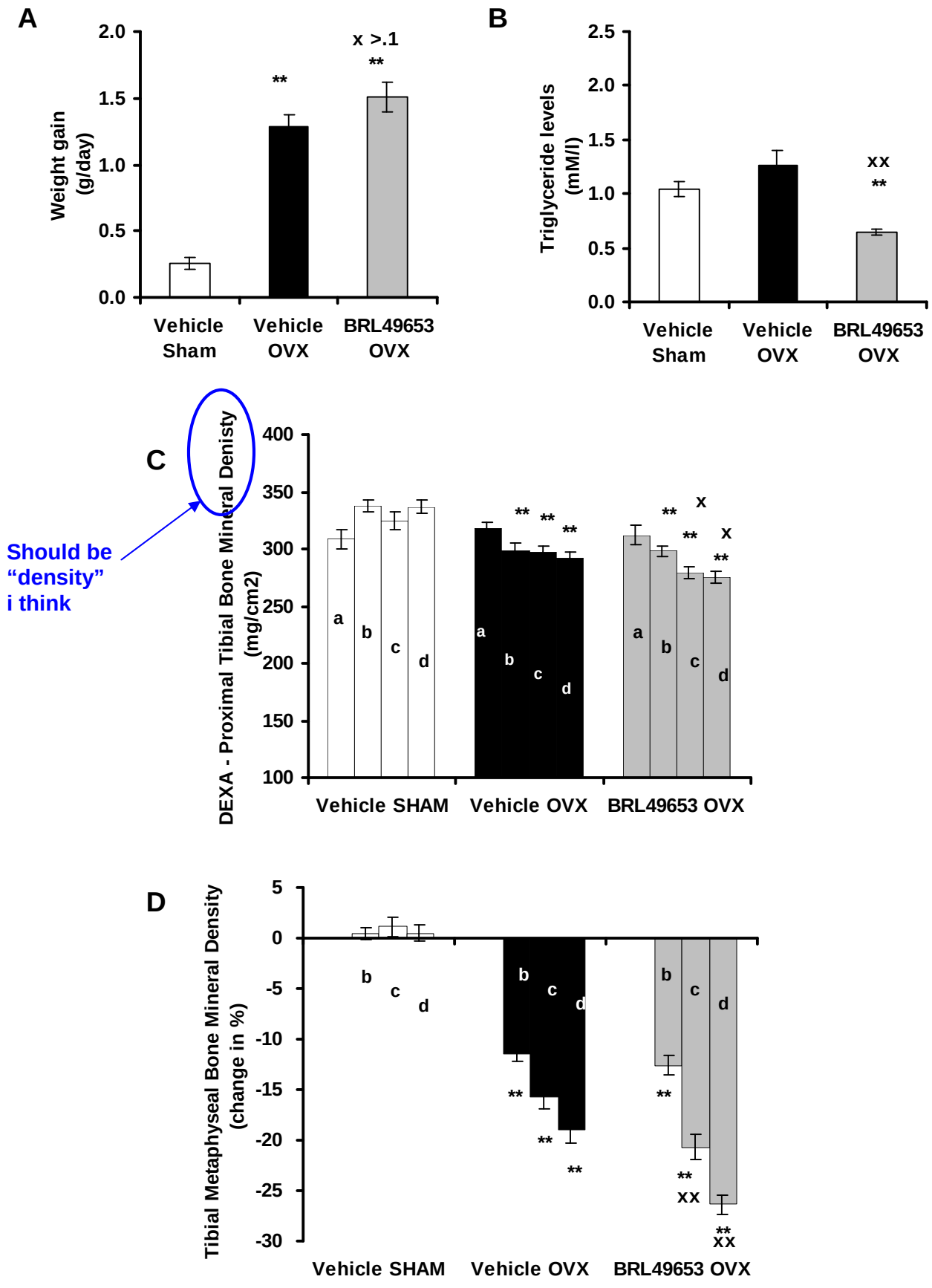
A
Weight gain (g/day)
2.0
1.5
1.0
0.5
0.0
**
x >.1
**
Vehicle Sham
Vehicle OVX
BRL49653 OVX
B
Triglyceride levels (mM/l)
2.5
2.0
1.5
1.0
0.5
0.0
xx
**
Vehicle Sham
Vehicle OVX
BRL49653 OVX
C
Should be "density" i think
DEXA - Proximal Tibial Bone Mineral Denisty (mg/cm2)
400
350
300
250
200
150
100
a
b
c
d
**
x
Vehicle SHAM
Vehicle OVX
BRL49653 OVX
D
Tibial Metaphyseal Bone Mineral Density (change in %)
5
0
-5
-10
-15
-20
-25
-30
b
c
d
**
xx
Vehicle SHAM
Vehicle OVX
BRL49653 OVX

Figure 6

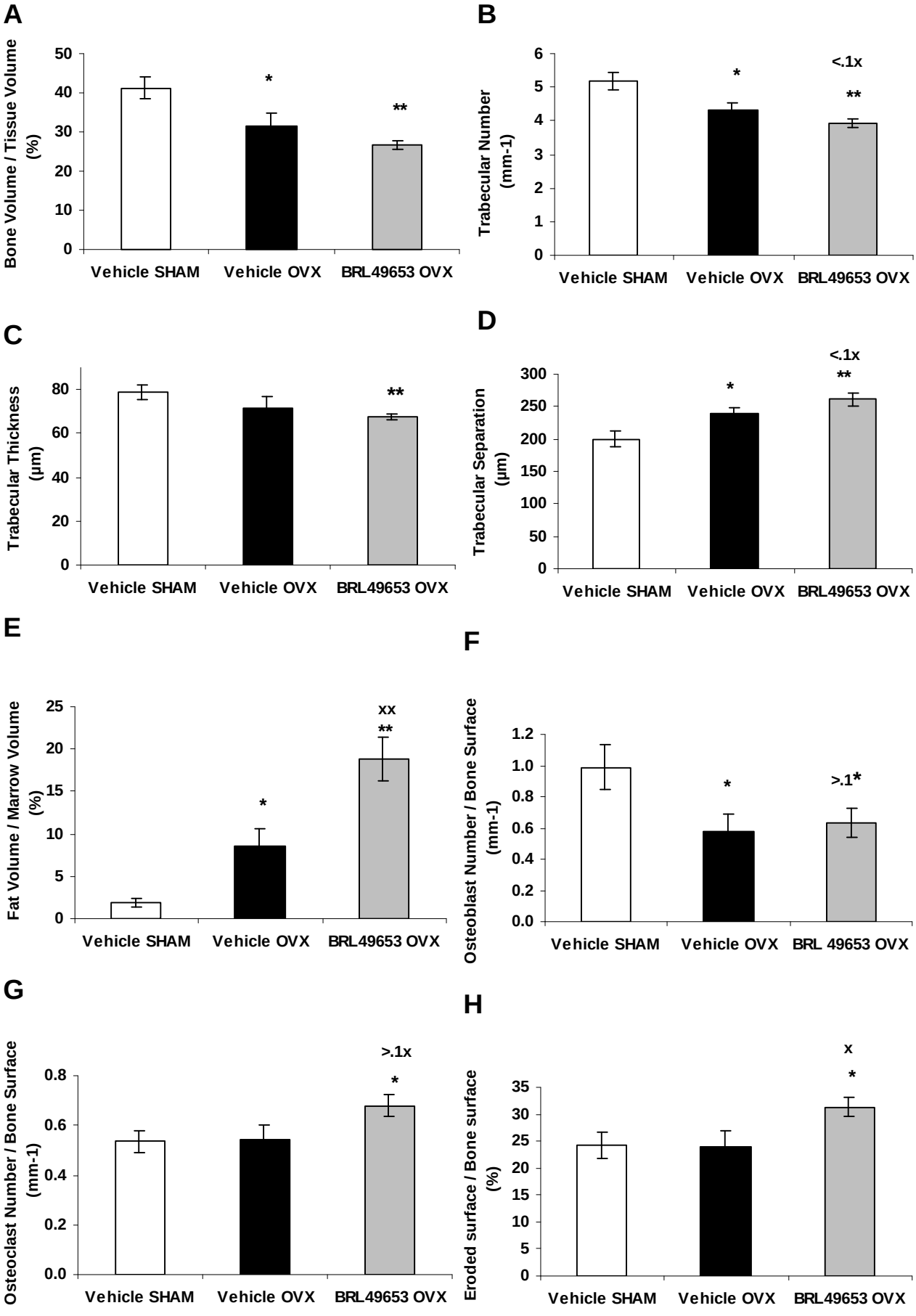
A
Bone Volume / Tissue Volume (%)
50
40
30
20
10
0
*
**
Vehicle SHAM
Vehicle OVX
BRL49653 OVX
B
Trabecular Number (mm-1)
6
5
4
3
2
1
0
*
<.1x
**
Vehicle SHAM
Vehicle OVX
BRL49653 OVX
C
Trabecular Thickness (µm)
80
60
40
20
0
**
Vehicle SHAM
Vehicle OVX
BRL49653 OVX
D
Trabecular Separation (µm)
300
250
200
150
100
50
0
*
<.1x
**
Vehicle SHAM
Vehicle OVX
BRL49653 OVX
E
Fat Volume / Marrow Volume (%)
25
20
15
10
5
0
*
xx
**
Vehicle SHAM
Vehicle OVX
BRL49653 OVX
F
Osteoblast Number / Bone Surface (mm-1)
1.2
1.0
0.8
0.6
0.4
0.2
0.0
*
>.1*
Vehicle SHAM
Vehicle OVX
BRL 49653 OVX
G
Osteoclast Number / Bone Surface (mm-1)
0.8
0.6
0.4
0.2
0.0
>.1x
*
Vehicle SHAM
Vehicle OVX
BRL49653 OVX
H
Eroded surface / Bone surface (%)
35
30
25
20
15
10
5
0
x
*
Vehicle SHAM
Vehicle OVX
BRL49653 OVX

Figure 7